The Energy Consumption Comparison of Temperature Difference-based Defrosting Exit Method and Time-based Defrosting Exit Method with Various Static Pressure Differences

Wu Yufan[1], Li Chao[1,*], Xu Wenjuan[2], Wan Yong[2], Zhao Yiji[2] and Song Zilong[1]

[1]*College of Mechanical and Electrical Engineering, Chengdu University of Technology, Chengdu 610059*

[2]*Sichuan Academy of Agricultural Machinery Sciences, Chengdu 610066*

Abstract: The time-based defrosting exit method(TDEM) has been widely used in cold storage, but the issue of energy consumption has been heavily criticized. In this paper, a temperature difference-based defrosting exit method(TDDEM) is proposed to compare with TDEM. Firstly, a parameter acquisition system of cold storage is constructed, and the experimental setup is conducted to determine the experimental parameters. Subsequentially, the range of defrosting static pressure difference is determined based on pre-frosting experiment, and the defrosting experiment of TDEM and TDDEM are carried out at five various static pressure difference conditions, 16Pa, 14Pa, 12Pa, 10Pa and 8Pa, respectively. The results show that the temperature fluctuations per defrosting events of TDEM are more severe compared to TDDEM, with with average increases of 102.2%, 91.6%, 59.3%, and 46.5%, respectively. Energy consumptions of TDDEM are markedly lower than TDEM, with reductions of 21.4%, 15.7%, 14.09% and 14.59%, respectively. Whether TDEM or TDDEM, the lowest energy consumption is occurred at 10Pa, and highest is 8Pa.

Keywords: Energy consumption, Cold storage, Static pressure difference, Temperature difference, Defrosting exit method.

1. INTRODUCTION

Studies have shown that 40% of food needs to be refrigerated, which uses 11% of total electricity [1], causing substantial energy waste. Thus, studying energy-saving technologies for small cold storage is crucial for conserving energy and protecting the environment. Current research on energy saving for small cold storage includes new refrigerants, energy-efficient control systems, and peak-shaving techniques. Scholars also focus on energy-saving defrosting control technologies.

Timed defrosting, as one of the earliest defrosting control methods, has been proven to be inaccurate [2-4]. It lacks real-time detection of evaporator frosting, failing to determine the optimal defrosting timing. The same goes for time-based defrosting exit method(TDEM), where excess defrosting time leads to wasted energy consumption. Beyond this, other defrosting control methods include: (1) Indirect measurement method, which measures the thickness of the frost layer indirectly through sensor values. Wei W *et al*. [5] combined temperature and time for defrosting control. This method is relatively simple and low-cost, but it cannot adapt to varying frosting conditions and is easily affected by humidity fluctuations, which impairs the precision of defrosting. Zhu j *et al*. [6] compared the traditional temperature-time method with a novel temperature-humidity-time defrosting control strategy that considers humidity, enhancing the precision of defrosting. The pressure difference defrosting control method is a relatively more accurate defrosting control method. Scholars [7-9] have validated the reliability of the pressure difference defrosting control method. However, the initiation static pressure difference for defrosting is primarily determined by visual assessment of frosting levels, neglecting energy-saving considerations. To address this, Junda Z *et al*. [10] proposed a dimensionless parameter, the pressure loss factor (PLF), based on pressure difference sensors to determine the start time of defrosting.Their experimental results show that this method is more accurate. Additionally, Scholars [11-14] have installed parallel plate capacitors between the evaporator fins to measure frost thickness through capacitance feedback, implementing a defrosting control method based on capacitance thresholds. But foreign objects may enter capacitors, which may cause misjudgment. This method assesses only local frosting on evaporator fins. (2) Direct measurement method. Scholars [15-17] have installed cameras behind the evaporator fins to visualize the frosting degree of the evaporator, which to some extent improves the accuracy of defrosting initiation and reduces the energy consumption of the cold storage. However, this method is costly, and the optical systems such as lenses are susceptible to interference at low temperatures. (3) Intelligent defrosting control method. By inputting parameters into a neural network, a predictive model based on a specific algorithm is established. This method determines the start and end points of defrosting, optimizing the automatic control of the defrosting process. For example, scholars [18-19] have

*Address correspondence to this author at the College of Mechanical and Electrical Engineering, Chengdu University of Technology;
Tel: +86 18202822945; E-mail: lichao19@cdut.edu.cn.

established models for unit failure, frosting prediction, and defrosting duration using BP algorithm with specified defrosting parameters. These models have been applied to defrosting control, confirming their predictive accuracy. Zhao *et al*. [20] proposed an evaluation method for frosting degree that combines fractal dimension with heat output decay. Concurrently, they developed an optimized YOLOv5-frost network, enhancing the accuracy of frosting detection through iterative training. Although this category of methods may exhibit good energy-saving performance for a specific cold storage, their development process is complex and they lack universal applicability.

In summary, scholars have conducted extensive research on various defrosting methods, which have been applied to some extent. However, the initiation threshold of existing pressure difference defrosting technology is mostly based on experience, and the defrosting exit method is mostly (TDEM). Although the fact that scholars have confirmed that the frost layer is completely removed when the trend of the temperature difference between the evaporator's inlet and outlet changes [21], research on the energy-saving aspects of this defrosting exit method is relatively lacking. To address this, this paper selects the difference between the evaporator inlet air pressure and the static air pressure within the cold storage as the defrosting initiation parameter, which is referred to as the static pressure difference in subsequent sections. A data acquisition and a control system of cold storage are constructed for continuous defrosting experiments. Under the premise of using TDEM, this paper analyzes the defrosting frequency, energy consumption, temperature fluctuations in the cold storage, and changes in the cooling effect of the unit when defrosting is initiated at various static pressure differences. Additionally, a contrast experiment is established to dynamically control defrosting time using temperature difference-based defrosting exit method(TDDEM), aiming to explore its energy-saving capabilities. This paper aims to provide a reference for further advancing energy conservation and emission reduction in cold storage facilities.

2. EXPERIMENTAL PRINCIPLE

2.1. Effect of Frosting on Air Pressure at the Back of Evaporator

The following equation represents the Bernoulli equation for ideal gases under isothermal conditions, as derived by Yue Z *et al*. [22]:

$$\frac{1}{2}v^2 + U + \frac{p}{\rho}\ln\frac{p}{p_0} = C \tag{1}$$

Equation (2) indicates that lower air velocities result in higher pressures. During the normal operation of the evaporator, the air velocity at the inlet is greater than the air velocity at rest within the storage. Consequently, the pressure at the inlet is lower than the pressure of the static air inside the cold storage. The air resistance increases and the wind speed decrease when the evaporator fins are blocked by frost. This causes an increase in the pressure at the evaporator inlet, reducing the difference between the inlet pressure and the pressure of the static air within the cold storage. This indicates that the static pressure difference can indirectly reflect the thickness of the frost layer. Consequently, this paper can use the static pressure difference as a basis for determining the initiation of defrosting.

2.2. Effect of Frost Formation on Heat Transfer Efficiency of Evaporator

Referring to the heat balance method of ASHRAE 75-77 Standard [23], the experimental cold storage is considered a closed system with a constant internal temperature. The cooling capacity of the evaporator can be determined by the following equation:

$$Q_A = \lambda\Delta t + Q_i \tag{2}$$

The heat transfer coefficient *K* of the evaporator fins can be determined by the following equation [24]:

$$Q_A = \frac{KA\Delta t\left(\theta_1 - \theta_2\right)}{\ln\left(\theta_1/\theta_2\right)} \tag{3}$$

Equation (3) shows that when frost adheres to the evaporator fins, a portion of the evaporator coil exchanges heat with the frost. The heat transfer area A between the fins and air decreases, reducing the cooling effect of the evaporator. It can also be inferred that the temperature difference across the coil's inlet and outlet changes when it exchanges heat with different media. Therefore, this paper can use the temperature difference across the evaporator coil's inlet and outlet as a parameter to determine the defrosting exit time.

3. EXPERIMENT

3.1. Experimental Setup

This paper has constructed a real-time operation parameter acquisition and control system for the cold storage. The system block diagram is shown in Figure **1**, and the control interface is shown in Figure **2**.

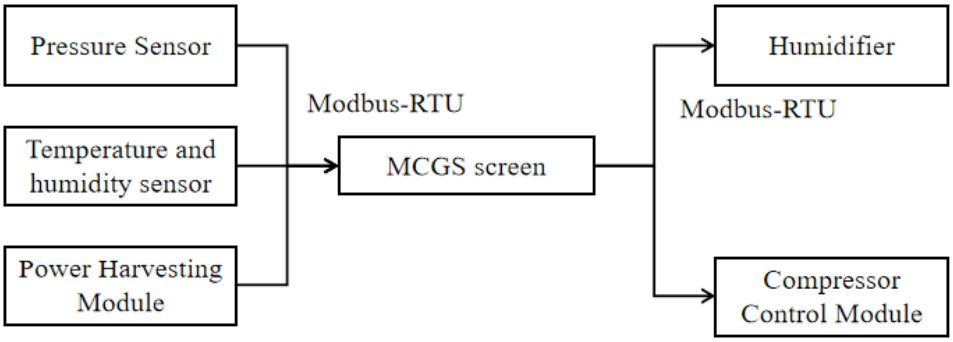

Figure 1: Structure of cold storage real-time Parameter acquisition and control system.

Figure 2: Control System Interface.

The cold storage is shown in Figure **3**(**a**) and Figure **3**(**b**). The specific sensor layout is shown in Figure **4** and Table **1**. The controllable parameters include set temperature, temperature fluctuation range, humidifier on/off, fan on/off, and defrosting initiation static pressure difference. During the experiment, no goods are stored in the cold storage. The evaporator is quickly frosted by humidifying with a humidifier.

Drawing from preliminary operational experience with the cold storage, the evaporator frosts more uniformly when the set temperature is -7°C, and the compressor start-stop frequency is more reasonable when the temperature fluctuation range is 1°C. Frosting is highly likely when the relative humidity within the storage exceeds 95% [7]. Consequently, the specific experimental conditions are set as follows: the set temperature is -7±1°C. The humidity in the cold storage is maintained above 95% at all times.

The following measures are adopted to enhance the accuracy of experimental data. As shown in Figure **4**(**e**), three temperature and humidity sensors are evenly positioned throughout the cold storage. Their average values are utilized as experimental parameters. All experiments commence when the temperature in cold storage reaches 25°C. Daily outdoor average temperatures are consistent during the experiments. When the humidity reaches 95%, the unit and humidifier are activated and humidification is maintained at a constant rate.

3.2. Defrosting Static Pressure Difference Range

A pre-frosting experiment must be conducted first to determine the appropriate range for the defrosting static pressure difference. The set temperature and temperature fluctuation range are configured in the control system, followed by the activation of the unit and humidifier. Due to the low-temperature and high-humidity environment, the frosting rate on the

(**a**) Exterior of the cold store (**b**) Inside the cold store

Figure 3: The cold store.

(**a**) Electricity metering modules

(**b**) Differential Pressure Sensor

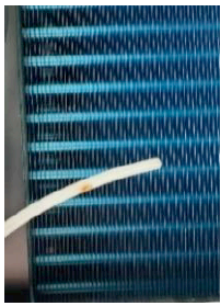

(**c**) Pressure detection position A

(**d**) Pressure detection position B

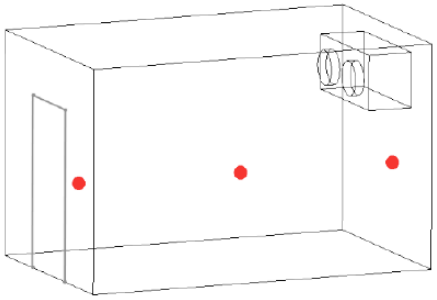

(**e**) Temperature detection position

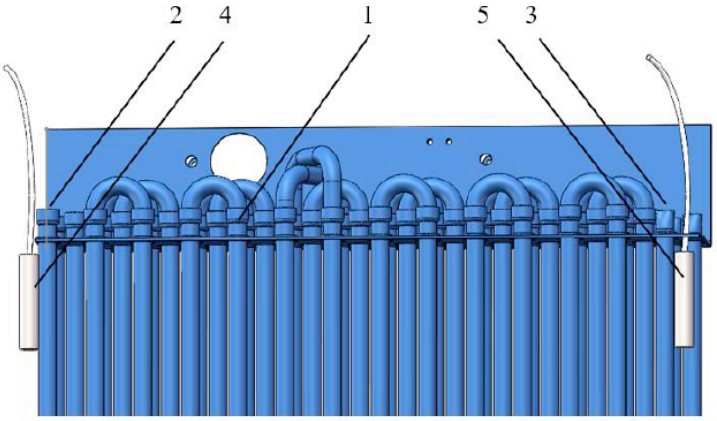

1. Evaporator coil 2. Coil inlet 3. Coil outlet 4. Temperature sensor A 5. Temperature sensor B

(**f**) Evaporator coil inlet and outlet temperature collection

Figure 4: Sensor position.

Table 1: Deployment of Sensors

Sensors	Function	Position of Distribution
Temperature and humidity sensor(±0.5℃、±1%RH)	Measure the temperature and humidity	Three points of uniform distribution inside the cold storage
Temperature sensor(±0.5℃、±1%RH)	Measure the temperature	Inlet and outlet of evaporator coil
Pressure sensor(±0.5pa)	Measure the static pressure difference	Evaporator inlet and where the air in the cold storage is stationary
Power Harvesting Module	Measure unit current and cumulative power consumption	Unit power input

evaporator fins will increase. The corresponding static pressure difference over time is shown in Figure **5**.

Observing the frosting process, it is noted that the static pressure difference is 24Pa when the evaporator

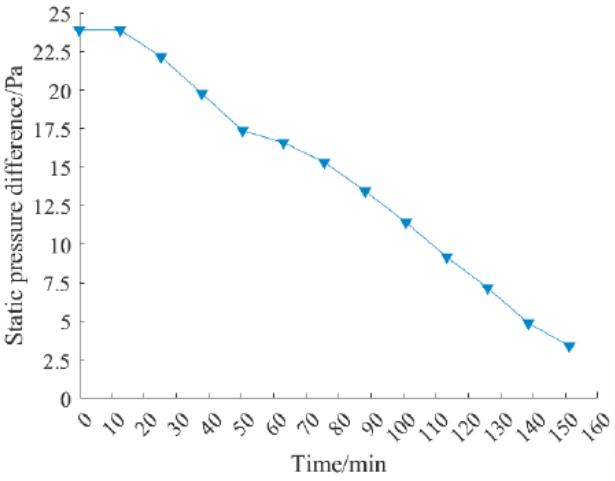

Figure 5: Change of the static pressure difference.

fins are completely free of frost. When the static pressure difference is 16Pa, as shown in Figure **6**(**a**), the fin end surfaces are almost completely covered with frost, but the frost layer between the fin gaps is extremely thin. When the static pressure difference is 8Pa, as shown in Figure **6**(**b**), the fin gaps are significantly blocked by the frost layer. When the static pressure difference is 4Pa, as shown in Figure **6**(**c**), the fins are completely covered by the frost layer, severely affecting the unit's cooling performance. Analyzing the frosting rate, it is observed that between 16 and 55 minutes of the experiment, the static pressure difference decreases from 24Pa to 16Pa, indicating the highest rate of decrease, *i.e*., the fastest frosting rate. When the static pressure difference is 8Pa, the frosting area on the evaporator fins is substantial, leading to a noticeable extension of the compressor's cooling time.

3.3. The Defrosting Experiment with TDDEM and TDEM

Two successive defrosting experiments groups using different defrosting exit methods (TDDEM and TDEM) are set up. In each experimental group, the cold storage is operated under various defrosting static pressure differences. To prevent false defrosting due to fluctuations in air pressure, the unit initiates defrosting when the static pressure difference reaches the set value and remains constant for 10 seconds.

The upper limit of the defrosting initiation static pressure difference is set at 16Pa to prevent excessive defrosting in experiments. When the static pressure difference falls below 8Pa, the cooling performance of the unit significantly declines, hence the lower limit for defrosting initiation static pressure difference is set at 8Pa. Within this range, a set of experiments are conducted every 2Pa. The defrosting static pressure differences of the contrast experiment are determined as: 16pa, 14pa, 12pa, 10pa and 8pa. There are five experiments for each of the two defrosting exit methods.

To ensure uniformity of experimental variables, the defrosting duration for the TDEM experimental group is set to the effective defrosting time corresponding to a static pressure difference of 8Pa. This is because the frosting degree is most severe at this value, requiring the longest time to completely remove the frost. Consequently, a defrosting experiment is first conducted at a static pressure difference of 8Pa.

Analyzing Figure **7**, it is observed that the temperature difference across the evaporator coil's inlet and outlet generally increases over the interval from 0 to 850 seconds. This is because as the gas reaches the coil outlet, the temperature approaches the freezing point of water, causing the temperature difference to continue to rise. After approximately 850 seconds, the temperature difference begins to decrease, which is attributed to the complete melting of the frost layer, allowing the hot gas within the coil to directly exchange heat with the cold, moist air inside the storage. The change in heat transfer medium leads to a change in the trend of temperature difference, indicating that defrosting should be halted. To ensure defrosting is complete, the TDEM experimental group sets the defrosting duration to 900 seconds per cycle, while the TDDEM experimental group ceases defrosting immediately after a continuous decrease in temperature difference for 50 seconds. Furthermore, to

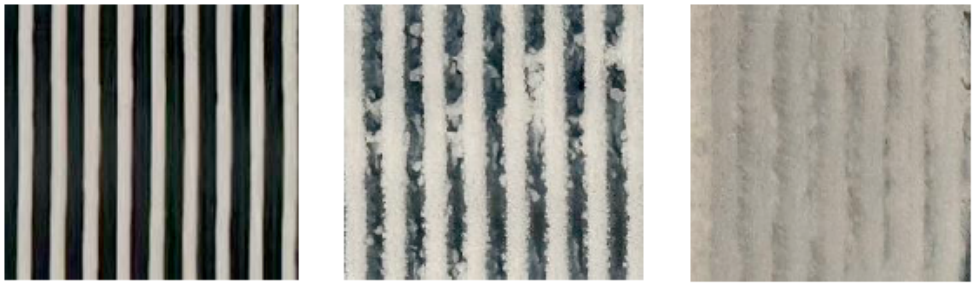

(**a**) 16Pa (**b**) 8Pa (**c**) 4Pa

Figure 6: Degree of fin frosting at various static pressure differences.

prevent the residual liquid water on the fins from refreezing into frost after defrosting, a 300-second drip time is set following the completion of defrosting. Experimental control parameters are shown in Table **2**.

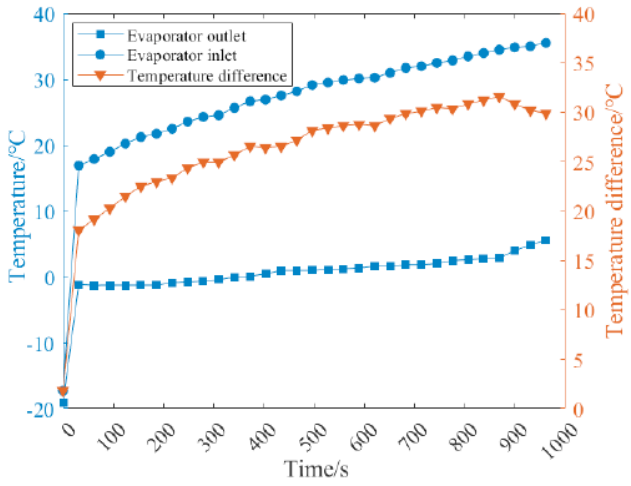

Figure 7: Curve of the difference between the outlet and inlet temperature of the defrost evaporator coil starting with a static pressure difference of 8 Pa.

4. EXPERIMENTAL RESULTS

4.1. Number of Defrostings and Accumulated Time

As shown in Figure **8**, the defrosting static pressure differences are set at 16Pa, 14Pa, 12Pa, 10Pa and 8Pa, respectively, for both defrosting exit methods, and their defrosting frequencies and accumulated defrosting times are presented. As shown in Figure **8**(**a**), within 8 hours, the number of defrostings for TDEM are 7, 6, 6, 5 and 3, the number of defrostings for TDDEM are 8, 7, 7, 5 and 3. As shown in Figure **8**(**b**), the cumulative defrosting time for the TDDEM are 47.8%, 63.2%, 73.6%, 76.8% and 96.8% of those for the TDEM. It is evident that within the same duration, the higher the set static pressure difference with TDEM, the greater the cumulative defrosting time and the increasing trend in defrosting frequency. When TDDEM is employed, the cumulative defrosting time is shorter compared to TDEM, eliminating unnecessary defrosting periods and enhancing the precision of defrosting.

Table 2: Experiment Parameters

Controls Parameter	Set Value
Set temperature	-7±1℃
static pressure Difference to start defrosting	16pa、14pa、12pa、10pa、8pa
Temperature outside the cold storage	25℃
Humidity in the cold storage	Continuous humidification from 95% at the same rate
The unit running duration	8h
Single defrosting duration(TDEM experimental group)	900s
Single defrosting duration(TDDEM experimental group)	Defrosting is terminated immediately after a continuous decrease in temperature difference for 50s.
Drip duration	300s

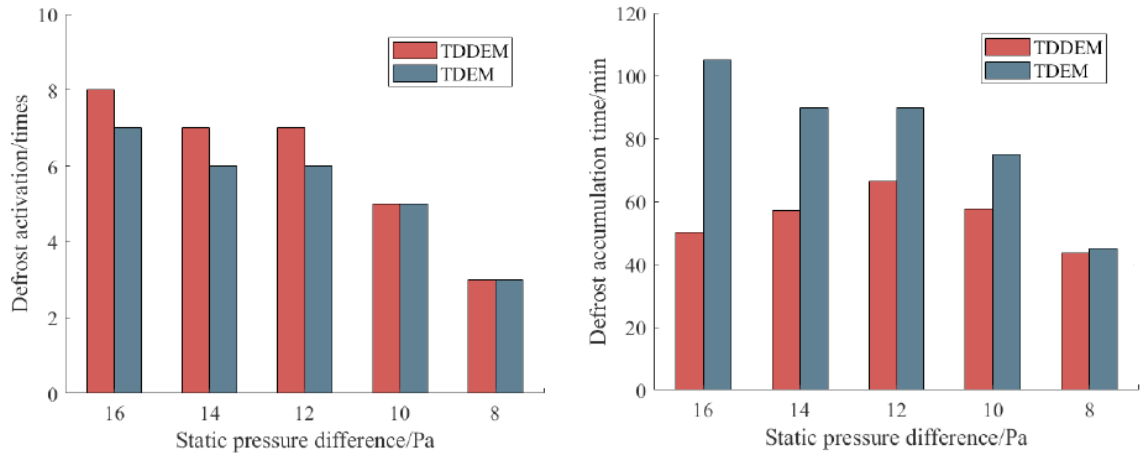

(**a**) Number of defrost activations

(**b**) Defrost accumulation time

Figure 8: Number of defrost activations and accumulated time.

4.2. Cold Storage Temperature and Refrigeration Efficiency

As shown in Figure **9**, each defrosting operation results in a significant increase in the average cold storage temperature. Because the evaporator stops cooling and passes hot gas while defrosting. Comparing the TDEM to the TDDEM at 16Pa, 14Pa, 12Pa and 10Pa for initiating defrosting, TDEM shows a markedly higher temperature increase per defrosting event, with averages 102.2%, 91.6%, 59.3% and 46.5% higher, respectively. At 8Pa for initiating defrosting, the temperature fluctuations between the two methods are nearly identical. Furthermore, after a

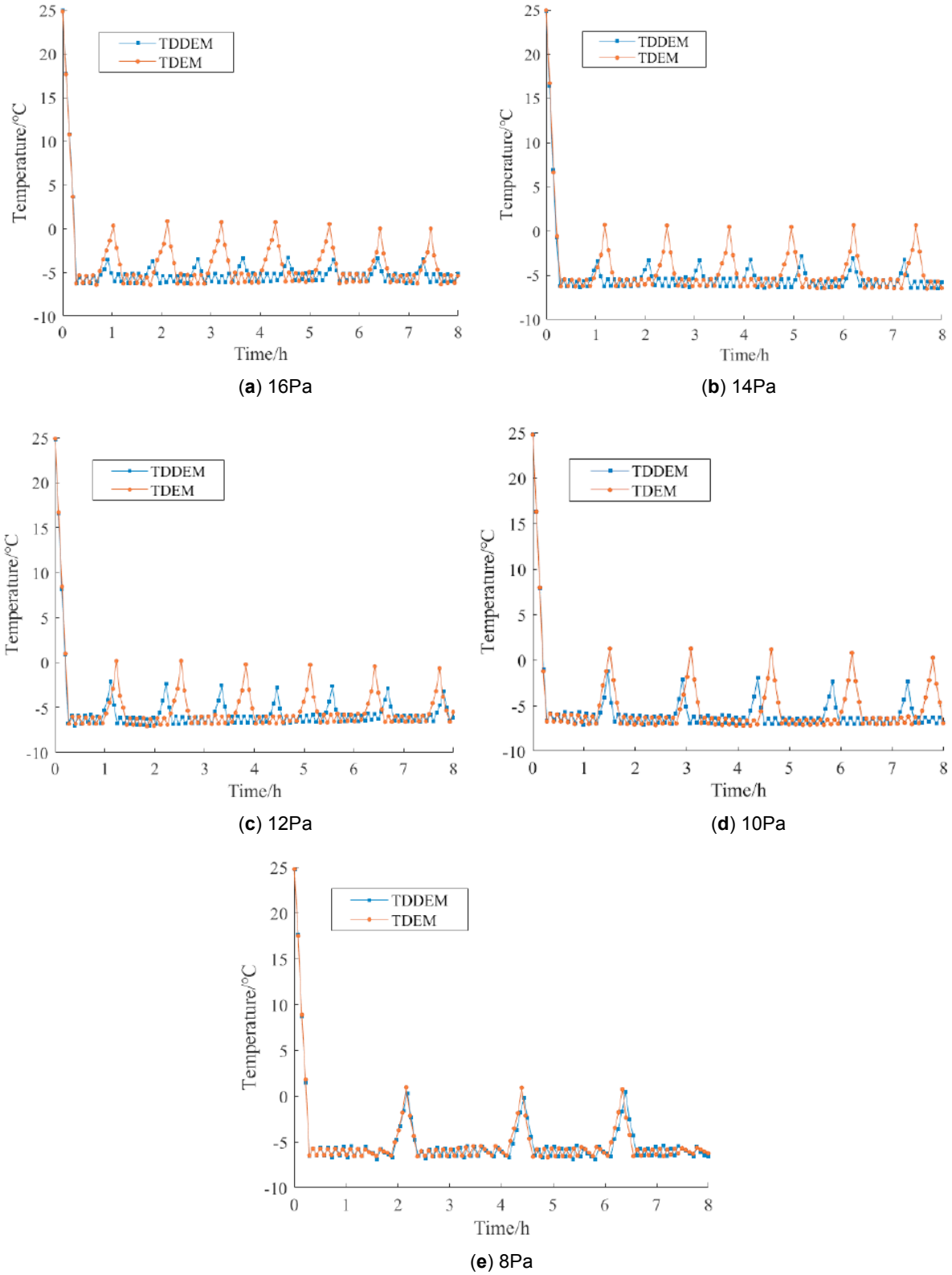

(**a**) 16Pa

(**b**) 14Pa

(**c**) 12Pa

(**d**) 10Pa

(**e**) 8Pa

Figure 9: Average temperature fluctuation of the cold storage.

period of refrigeration, the cold storage temperature takes longer to reach the set point, indicating a significant reduction in the cooling efficiency of the refrigeration unit. As shown in Figure **10**, the average cooling time per cycle with the defrosting static pressure difference set at 8Pa is significantly higher than in the previous four groups, potentially leading to increased energy consumption.

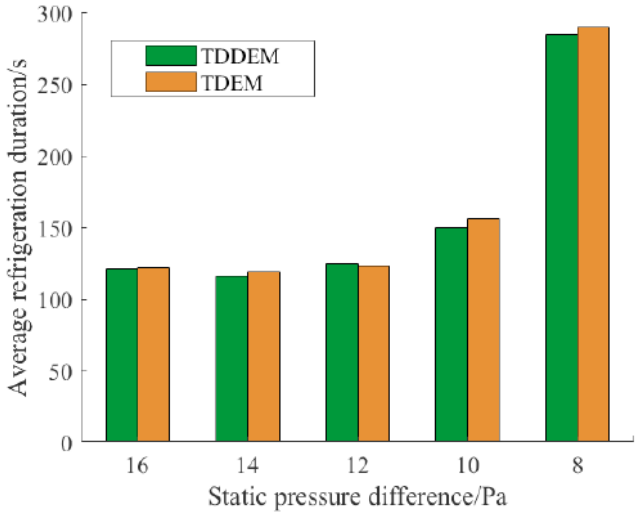

Figure 10: Average single cooling time when defrosting is activated at different static pressure difference.

4.3. Energy Consumption

As shown in Figure **11**, TDEM experiment group is designated as Group A, TDDEM experiment group is designated as Group B. Analyzing Group A, the overall energy consumption of the cold storage decreases as the defrosting static pressure differences are set at 16Pa, 14Pa, 12Pa and 10Pa, respectively. This is because the refrigeration unit maintains good cooling performance under these four defrosting initiation conditions. When the defrosting static pressure difference is set at 8Pa, the energy consumption peaks. The reason is that the evaporator fins become severely frosted for a portion of the time, which significantly impairs the unit's cooling efficiency, extends the cooling duration, and increases energy usage. Analyzing Group B, the trend in energy consumption mirrors that of Group A. However, compared to Group A, Group B exhibits a significant reduction in energy consumption when the defrosting static pressure differences are set at 16Pa, 14Pa, 12Pa and 10Pa, with reductions of 21.4%, 15.7%, 14.09% and 14.59%, respectively. This is due to the elimination of unnecessary defrosting time in Group B. The energy consumption is similar for both groups when the defrosting static pressure difference is set at 8Pa.

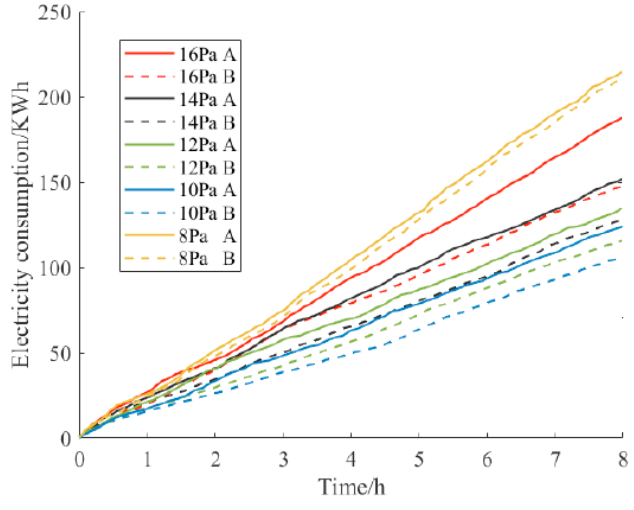

Figure 11: Power consumption-time diagram.

5. CONCLUSION

This paper investigates energy consumption comparison of TDDEM and TDEM through experimental method. The following conclusions can be drawn:

(1) For TDEM, the higher the defrosting static pressure difference, the more defrosting times there will be. The lower the defrosting static pressure difference, the less defrosting times there will be.

(2) Both TDEM and TDDEM, when the defrosting static pressure differences are set at 16Pa, 14Pa, 12Pa and 10Pa, there is no significant change in the single running time of the compressor. When the defrosting static pressure difference is set at 8Pa, the single running time of the compressor noticeably increases over time. This indicates the cooling performance of the unit declines sharply.

(3) When the defrosting static pressure differences are set at 16Pa, 14Pa, 12Pa and 10Pa, the temperature increases per defrosting event of TDEM are significantly higher than that of TDDEM, with average increases of 102.2%, 91.6%, 59.3% and 46.5%, respectively. However, when the defrosting static pressure difference is set at 8Pa, the temperature fluctuations between TDEM and TDDEM are similar.

(4) When the defrosting static pressure differences are set at 16Pa, 14Pa, 12Pa and 10Pa, the energy consumptions of TDDEM are respectively reduced by 21.4%, 15.7%, 14.09% and 14.59% compared to TDEM. When the defrosting static pressure difference is set at 8Pa, the energy consumptions are similar.

(5) Whether TDEM or TDDEM, the lowest energy consumption is occurred when the defrosting static pressure difference is set at 10Pa and highest is 8Pa.

CONFLICTS OF INTEREST

The author declared no conflicts of interest.

NOMENCLATURE

TDEM	time-based defrosting exit method
TDDEM	temperature difference-based defrosting exit method
v	gas flow velocity (m/s)
U	potential of the gas (J/kg)
p	gas pressure (Pa)
ρ	gas density (kg/m³)
p_0	atmospheric pressure (Pa)
C	constant
Q_A	evaporator cooling capacity (W)
λ	leakage coefficient (W/℃)
Δt	temperature difference between inside and outside of the cold storage (℃)
Q_i	heating capacity of the heater in the cold storage (W)
θ_1	temperature difference between the evaporator coil inlet and the cold storage (℃)
θ_2	temperature difference between the evaporator coil outlet and the cold storage (℃)
A	heat transfer product between the fins and the air (m²)

REFERENCE

[1] Jiang S, Ye S, Hanfei Q, *et al*. Research Progress on New Technology of Energy Saving and Emission Reduction in Perishable Food Refrigeration Chain [J]. Journal of Refrigeration, 2011, 32 (06): 69-73.

[2] Wang F, Wang Z, Zheng Y, *et al*. Performance investigation of a novel frost-free air-source heat pump water heater combined with energy storage and dehumidification [J]. Applied Energy, 2015, 139(feb.1): 212-219. https://doi.org/10.1016/j.apenergy.2014.11.018

[3] Xilong W. The Research of Continuous Defrosting of Refrigeration Storage [D]. Tianjin University of Commerce, 2017.

[4] Mengjie S, Cheng F, Ning M, *et al*. An experimental study on time-based start defrosting control strategy optimization for an air source heat pump unit with frost evenly distributed and melted frost locally drained [J]. Energy and Buildings, 2018, 178:26-37. https://doi.org/10.1016/j.enbuild.2018.08.027

[5] Wei W, Xu W, Yuying S, *et al*. Influence of different defrosting cycles on operating performance of air-source heat pumps [J]. Heating Ventilating & Air Conditioning, 2018, 48 (06): 1-7+60.

[6] Zhu J, Sun Y, Wang W, *et al*. A novel Temperature-Humidity-Time defrosting control method based on a frosting map for air-source heat pumps [J]. International Journal of Refrigeration, 2015, 54: 45-54. https://doi.org/10.1016/j.ijrefrig.2015.02.005

[7] Dengke H. Experimental Research on Defrosting of Cold Storage System Based on Frost Layer Visualization and Fuzzy PID Control [D]. Tianjin University of Commerce, 2023.

[8] Ruiting S, Experimental Study on the Effect of Reduction of Defrost Heat by the Top-mounted Cold Storage Plate on Temperature Field of Cold Storage [D]. Tianjin University of Commerce, 2017.

[9] Chung Y, Na S I, Choi J M, *et al*. Feasibility and optimization of defrosting control method with differential pressure sensor for air source heat pump systems [J]. Applied Thermal Engineering, 2019, 155: 461-469. https://doi.org/10.1016/j.applthermaleng.2019.04.002

[10] Junda Z, Huan S, Xinghua L, *et al*. Theoretical and experimental research on a new defrosting control strategy based on differential pressure sensor [J]. International Journal of Refrigeration, 2022, 143: 11-18. https://doi.org/10.1016/j.ijrefrig.2022.06.031

[11] Zheng X, Shi R, You S, *et al*. Experimental study of defrosting control method based on image processing technology for air source heat pumps [J]. Sustainable Cities and Society, 2019, 51: 101667. https://doi.org/10.1016/j.scs.2019.101667

[12] Malik A N, Khan S A, Lazoglu I. A novel demand-actuated defrost approach based on the real-time thickness of frost for the energy conservation of a refrigerator [J]. International Journal of Refrigeration, 2021 (131-): 131. https://doi.org/10.1016/j.ijrefrig.2021.07.032

[13] Yuchen S, Haoyang Z, Sophie W. Detection of frost growth and distribution on louver and offset strip fins of a microchannel heat exchanger using capacitance sensing approach [J]. International Journal of Heat and Mass Transfer, 2023, 217. https://doi.org/10.1016/j.ijheatmasstransfer.2023.124650

[14] Qi W. Research on Intelligent Defrosting Control Based on the Principle of Parallel Plate Capacitors[D]. Tianjin University of Commerce, 2023.

[15] Yong H. Research on Defrosting Control Method of Air Source Heat Pump Based on Image Processing Technology [D]. Tianjin University, 2018.

[16] Dazhen Y. Defrosting Control Method of Air Source Heat Pump Based on Fractal Theory for Image Recognition [D]. Tianjin University, 2018.

[17] Miao H, Yang X, Yin D, *et al*. A novel defrosting control strategy with image processing technique and fractal theory [J]. International Journal of Refrigeration, 2022,138:259-269. https://doi.org/10.1016/j.ijrefrig.2022.03.002

[18] Jiang S, Wei D, Pengcheng X. Research on Defrost Control of Cold Storage Cooling Fan Based on Neural Network Model [J]. Fluid Machinery, 2020, 48 (04): 72-77.

[19] Pengcheng X. Research on Automatic Defrost Control Strategy Based on Intelligent Algorithm [D]. Tianjin University of Commerce, 2019.

[20] Zhao H, Li P, Li J, *et al*. Applying neural network model to real-time frosting detection and intelligent defrosting control for air source heat pump [J]. Applied Energy, 2025, 377 (PA): 124444-124444. https://doi.org/10.1016/j.apenergy.2024.124444

[21] Lulu N, Qingjiang L, Xilong W. End time of continuous hot gas defrosting in small cold storage [J]. Refrigeration and Air-Conditioning, 2022, 22 (04): 54-57.

[22] Yue Z, Guofeng Z. A Discussion on The Bernoulli's Equation of Ideal Gas under Isothermal Condition [J]. Physics and Engineering, 2021, 31 (01): 22-24.

[23] Society of Heating, Refrigeratingand Air-Condi-Americantioning Engineers. ASHRAE handbook [M]. Atanta, Ga: American Society of Heating, Refrigerating and Air Conditioning Engineers, 2017.

[24] Jie P, Zhili S, Yabo S, *et al*. Experimental Research on Heat Transfer Performance of Single-tube Multi-row Finned Tube Evaporator [J]. Journal of Refrigeration, 2022, 43 (01): 116-122.

Received on 05-11-2024 Accepted on 02-12-2024 Published on 04-12-2024

https://doi.org/10.31875/2410-2199.2024.11.08